CHEMICAL ENGINEERING TRANSACTIONS
VOL. 70, 2018
A publication of AIDIC
The Italian Association of Chemical Engineering
Online at www.aidic.it/cet
Guest Editors: Timothy G. Walmsley, Petar S. Varbanov, Rongxin Su, Jiří J. Klemeš

ISBN 978-88-95608-67-9; **ISSN** 2283-9216
DOI: 10.3303/CET1870179

Study of Continuous Corrosion on ASTM A335 P91 Steel in an Environment of CO_2-O_2-N_2-H_2O Derived from the Theoretical Combustion Products of a Mixture of Refining Gases at High Temperatures

Anibal Alviz-Meza[a,*], Javier A. Sanabria-Cala[b], Viatcheslav Kafarov[a], Dario Y. Peña-Ballesteros[b]

[a]Centro de Investigación para el Desarrollo Sostenible en Industria y Energía, Universidad Industrial de Santander, Bucaramanga, Colombia. Ciudad Universitaria, Cra 27 No. 9, A.C. 680002, Colombia.
[b]Grupo de Investigación en Corrosión, Universidad Industrial de Santander, Bucaramanga, Colombia. Parque Tecnológico Guatiguará, Km 2 vía refugio, Piedecuesta, A.C. 681011, Colombia.
anibalalvizm@hotmail.com

The current energy production processes go hand in hand with corrosive phenomena; which is the case of combustion process in a refinery, where the presence of compounds such as CO_2 and H_2O, result in alloys catastrophic carburization and oxidation respectively. In this research work was evaluated the corrosive effect that can be generated in a real combustion environment, for which, it was necessary to select a model mixture of refinery gases and to simulate its theoretical combustions products. The main results showed the formation of a semi-protective duplex oxide layer; whose inner layer was composed mainly of chromium, while the outer layer was much richer in iron. On the other hand, the carburizing effect of CO_2 was suppressed by the high oxygen potential in the combustion environment; leading to the conclusion that in real conditions, at 750 ºC and after 200 h of testing, steels such as ferritic alloy ASTM A335 P91, could not present appreciable damages during their operation in refinery boilers and furnaces.

1. Introduction

The combustion of fossil fuels such as carbon, petroleum and natural gas; is fundamental for energy generation, nevertheless, these gases are characterized by their high content of hydrocarbons, which completely burned or not, generate a carbon activity in the environment in which they are contained. High carbon activities and environments with low oxygen potentials can carburise steels, as Peña-Ballesteros et al. (2012) demonstrated for Fe9Cr1Mo (P91) ferritic steel in a reduced combustion atmosphere with CH_4, CO, CO_2 and H_2, at 550, 650 and 750 ºC. Moreover, researchers such as Rouillard and Furukawa (2016) have studied carburization in other reduced oxygen environments, noting that in pure CO_2 is also possible to obtain internal carburization on P91 steel at 550 and 600 ºC.

Carburization and oxidation are the most important corrosion effects at high temperatures, which can promote changes in the properties of P91 steel, in a combustion environment without H_2S; the first affecting ductility and thermofluence of alloys and the second creating oxide layers to difficult ionic diffusion through the oxide/gas interface. When ferritic steels are corroded in an atmosphere rich in oxygen, the carburization effect is suppressed, this behaviour was recently shown by Alviz et al. (2017a) in a combustion environment with CO_2, O_2, N_2, H_2O and H_2S at 750 ºC. However, in the scientific literature there is little information about simultaneous oxidation-carburization process, in a combustion environment of CO_2, O_2, N_2 and H_2O on P91 steel.

On the other hand, this research follows the lines of the studies realized by Kafarov et al. (2015), where the eco-efficiency of the combustion process in a refinery was evaluated, having in consideration CO_2 emission and the adiabatic temperature in a furnace. In this opportunity, it was evaluated the security aspect, through the corrosion study of typical Colombian refinery steel and gases.

Please cite this article as: Alviz-Meza A., Sanabria-Cala J.A., Kafarov V., Pena-Ballesteros D.Y., 2018, Study of continuous corrosion on astm a335 p91 steel in an environment of co2-o2-n2-h2o derived from the theoretical combustion products of a mixture of refining gases at high temperatures , Chemical Engineering Transactions, 70, 1069-1074 DOI:10.3303/CET1870179

2. Materials and methods

The methodology applied was similar to one used by Alviz et al. (2017b) to study pure oxidation, in an environment also derived from a mixture of refinery gases.
The first step to evaluate the simultaneous oxidation-carburization effect on P91 steel was to obtain the combustion gases composition. For this, a mixture of refinery gases from an study realized by Saavedra et al. (2013), at the refinery of Barrancabermeja-Colombia was selected. Then, the composition of the theoretical combustion products were simulated through Aspen Hysys 8.6. Once having the experimental conditions, the composition of the steel and combustion gases, to determine the theoretical corrosion products with HSC Chemistry 5.1 was possible.
On the other hand, regard to the experimental part, coupons of P91 steel were introduced inside tubular furnaces by duplicate (dimensions of 15 mm x 10 mm x 2 mm), where they were exposed to the combustion atmosphere calculated before, at the experimental conditions selected.

Figure 1: Experimental setup: 1) Cylinder with Ar, 2) Cylinder with CO_2-O_2-N_2, 3) Flow valve, 4) Relief valve, 5) Pressure gauge, 6) Mass flow meter, 7) Humidifier temperature controller, 8) Humidifier, 9) Heating cord, 10) tubular electric furnace, 11) Furnace controller, 12) Reactor and coupons holder and 13) Gas and steam outlet

The experimental condition selected, were similar to real combustion process at Barrancabermeja's refinery; an atmospheric pressure and a range of temperatures between 450 and 750 ºC (radiation zone of the furnaces). Furthermore, the exposition times selected were 1, 10, 20, 50, 100 and 200 h; similar to those used by Peña-Ballesteros et al. (2012) for their combustion atmosphere, which can be useful to compare the kinetics results.
Regard to coupons preparation, they were sanded before testing from SiC sandpaper No. 180 to 600. Each coupon was subjected to ultrasonic cleaning in acetone during 10 min, dried and marked, as is recommended by standard ASTM G1 (ASTM, Standard Practice for Preparing, Cleaning, and Evaluating Corrosion Test Specimens, 2011). To characterize the results obtained, SEM-EDS, XRD, hardness, microhardness and optical microscopy techniques were applied. Finally, the kinetic study was carried out taking into account the dimensions of the coupons, as well as the mass gained by each one.

3. Results

3.1 Simulation results

3.1.1 Determination of combustion environment

Based on the average of the compounds of higher occurrence in a chromatographic study realized by Saavedra et al. (2013) at the refinery of Barranbermeja-Colombia, to obtain a model mixture of combustion gases was possible. Table 1 shows the molar composition calculated for the combustion gases.

Table 1: Molar composition of the combustion environment

Compounds	CO_2	N_2	O_2	H_2O
%Molar	9.131	72.394	1.749	16.726

The procedure to determinate the combustion environment composition was the same applied by Alviz et al. (2017b) to obtain their oxidation atmosphere.

Having in consideration the experimental design in Figure 1, the CO_2-N_2-O_2 mixture was humidifier into H_2O to obtain the complete combustion atmosphere; for this, a 0.02 kg/h flow mass value was supposed for the entire mixture. Through the total mass flow and a temperature of 298 K, a volumetric flow of 238.3 cm^3/min for CO_2-N_2-O_2 and a mass flow of 35.83 mg/min for water vapour were obtained.

3.1.2 Obtaining of theoretical corrosion products

Once determined the combustion molar composition at the experimental conditions, to obtain the equilibrium composition and phase stability diagrams were possible. Table 2 shows the elemental composition from the P91 supplied steel.

Table 2: Elemental weigh fraction of P91 steel

%Mo	%C	%Si	%Mn	%P	%S	%Ni	%Cr	%V	%Nb	%Al	%N	%Fe
0.989	0.106	0.768	0.316	0.013	0.003	0.271	8.439	0.024	0.008	0.006	0.015	89.042

Thermodynamic equilibrium was calculated using the experimental conditions of pressure and temperature, as well as the steel and combustion gases composition. This simulation gave the theoretical corrosions products, which can be observed in Figure 2. The molar steel/gas ratio used for this simulation in HSC Chemistry 5.1 was 1/1000, as is recommended by John (2010).

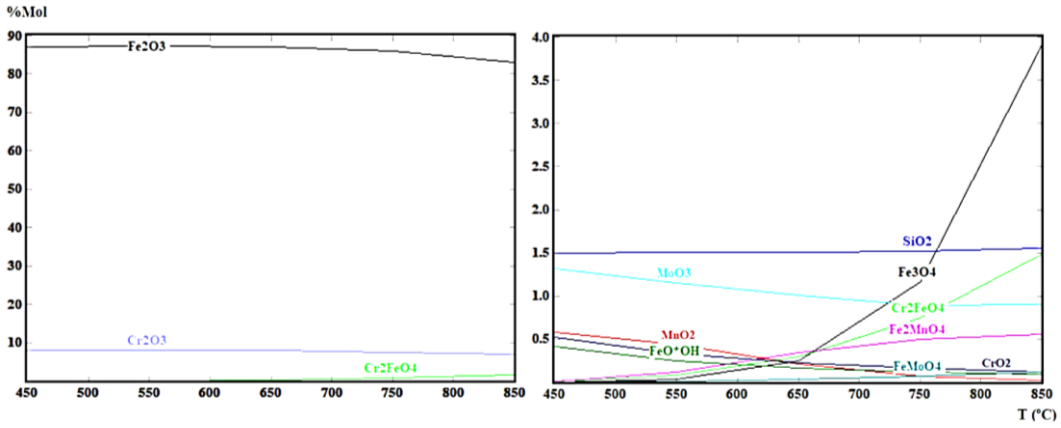

Figure 2: Variation of the Molar percentage from the simulated corrosion products against temperature

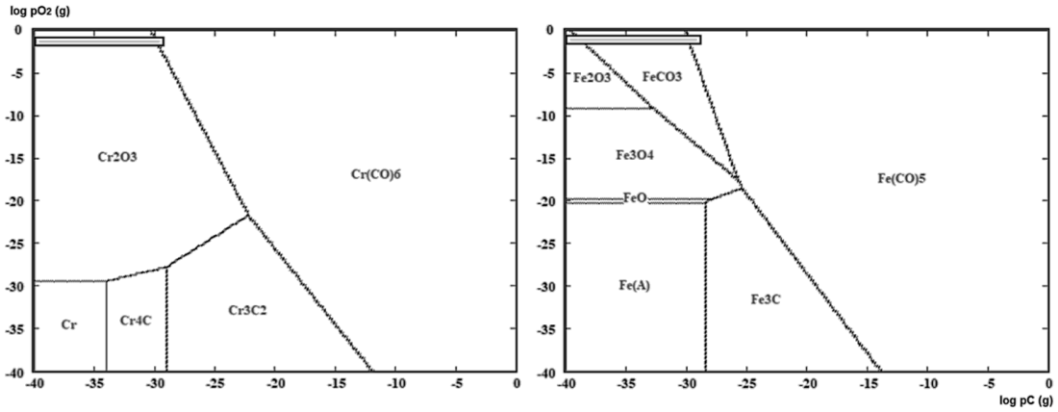

Figure 3: Cr-C-O and Fe-C-O Phase stability diagrams between 450 and 750 °C

The main result of the simulation showed that, for the selected experimental conditions, carburization is not thermodynamically favoured but oxidation does. The predominant oxides identified were: hematite, chromite, magnetite, silicon and molybdenum oxides, as well as two other spinels. This result can be explained by the high oxygen partial pressure in the environment, which suppresses carbides formation.
Otherwise, in order to appreciate the corrosion products that could be formed on P91 steel, according to oxygen partial pressure and carbon activity, the phase stability diagrams were constructed. Figure 3 shows the range

of values among which the carbon activity varies (following the bar at the top of the figure), for the calculated oxidation potential of $pO_2 = 1.749 \times 10^{-1}\ atm$, from the combustion environment. Then, the bar in Figure 3 shows the possible formation of chromite, hematite and siderite.

3.2 Experimental results

3.2.1 Metallographic analysis

Figure 4a, allows to appreciate a ferritic microstructure with a low content of lamellar perlite and a fine grain size, characteristic behavior of normalized and tempered manufactured P91 steels. After 200 h at 750 ºC, P91 matrix shows also a ferritic microstructure with a smaller clumping of pearlite at the grain boundaries. This is a typical behaviour when the carbon diffusive processes in the alloys increase. This behavior generates variations in the steel mechanical properties, reducing its resistance to stresses. In Figure 4b, is also possible to observe the formation of fine and thick carbide and carbonitrides precipitates; corresponding mainly to $M_{23}C_6$ and M_7C_6 carbides; with M as Cr, Fe, Mo, Nb and V.

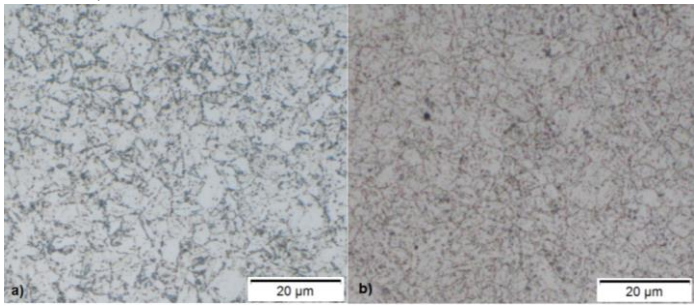

Figure 4: Optical microscopy (500 x) for P91 steel: a) before testing and b) after 200 h of testing at 750 °C

3.2.2 Hardness and microhardness analysis

In order to complement the metallographic analysis, hardness and microhardness tests were carried out. The results of comparing the initial hardness of the steel with its hardness after the longer exposure time, did not show significant changes; which implies the absence of internal corrosion, as would be the case of carburization. Regarding the analysis of microhardness, an irregular behavior was observed, however a slight increase can be generalized, related to the appearance of multiple precipitates in the metallic matrix. These results can be observed in Table 3.

Table 3: Hardness and microhardness analysis after 200 h of testing. The force applied by each analysis was 588.40 and 0.49 N respectively

	Initial state	450 ºC	550 ºC	650 ºC	750 ºC
Hardness (Rockweel A)	58	57.6	55.2	58.2	58.2
Microhardness (Vickers HV)	229.4	258.7	188.6	227.8	234.5

3.2.3 Scanning electron microscopy with x ray microanalysis

As can be seen in Figure 5, a duplex structure was found in the oxide layer; composed mainly of an iron-rich outer layer and an inner layer rich in chromium. These results were also reported by Martinelli et al. (2015), additionally, Rouillard and Furukawa (2016) took the job of characterizing the innermost layer by TEM-EDS technique, finding that its composition responds to the $Fe_{3-x}Cr_xO_4$ molecular formula. For its part, the outer layer, which is easier to characterize, has been reported as a layer rich in hematite and magnetite.

An important aspect in SEM images from Figure 6, is that oxide layers become more wide and imperfect with the increase in temperature. So, for higher temperatures, multiple cracks and voids begin to appear, more specifically, in the intermediate region between the $Fe_{3-x}Cr_xO_4$ spinel and the oxide/gas interface. This region is characterized as magnetite in many P91 oxidation studies, which is also a spinel but inverse $Fe^{II}O.Fe^{III}{}_2O_3$ (31 % FeO and 69 % Fe_2O_3), with good electrical conductivity properties.

The electrical conductivity of magnetite, allows it to act as a messenger of Fe cations between the chromium spinel and the oxide/gas interface, thus giving rise to hematite formation. Which is explained by the migration of Fe^{+3} cations from the intermediate layer to the gaseous interface, which is more abundant in this layer and with a lower ionic radio, making its diffusion easier and more viable. This continuous reaction between magnetite

and hematite, wears the intermediate layer, generating the appearance of large cracks and gaps. In addition, that behaviour is favoured by the presence of water vapour in the environment; which generates wastage in the oxide layers by the formation of volatile oxides, and the appearance of multiple empty spaces, which are taken by atomic hydrogen, as Perez and Castañeda (2006) suggest. When this phenomenon occurs, it is the exact moment for the appearance of carburization phenomena, being that carbon-free atoms diffuse more easily towards the metallic matrix; however, for this to happen, longer exposure times are needed.

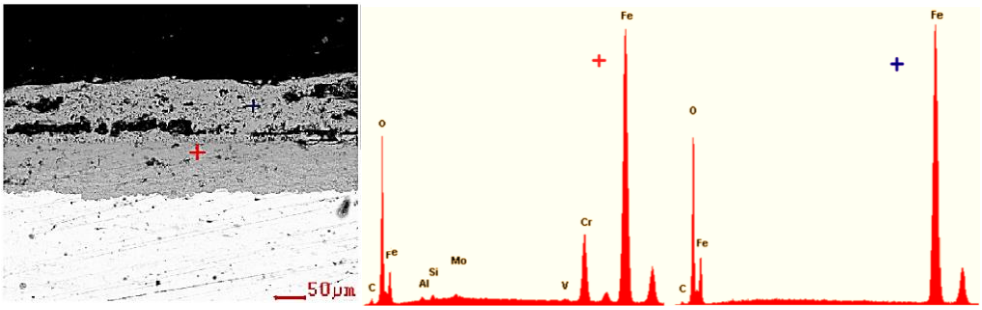

Figure 5: SEM-EDS from P91 sample after 200 h at 750 ºC

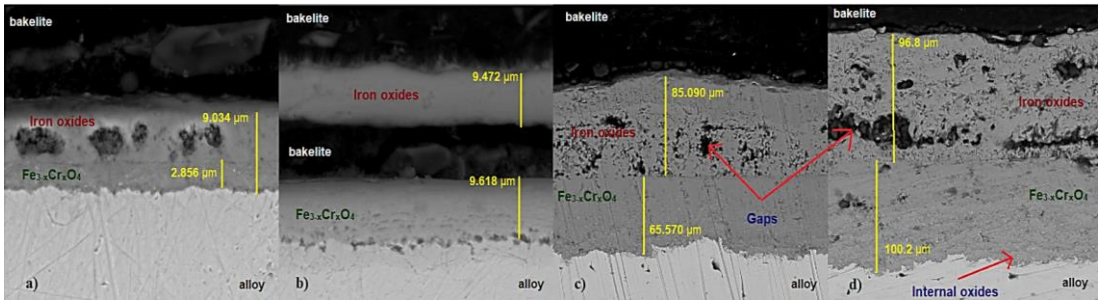

Figure 6: SEM images from P91 samples after 200 h of testing at: a) 450 ºC (5000 x), b) 550 ºC (5000 x), c) 650 ºC (1000 x) and d) 750 ºC (1000 x)

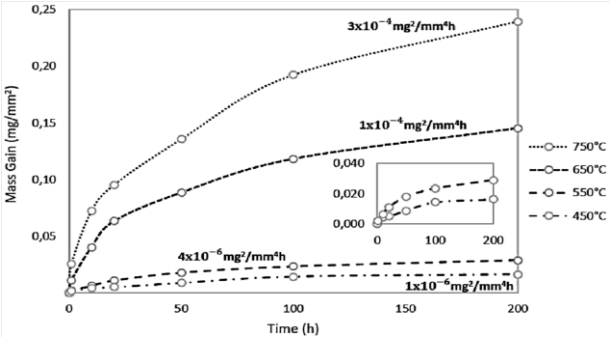

Figure 7: Mass gain against time and parabolic kinetic constants, obtained for the experimental conditions evaluated in the simulated combustion environment

3.2.4 X-ray diffraction analysis

Through x-ray diffraction analysis, the crystalline structures present at the oxide layer surface were determined, after 200 h of testing and for all the working temperatures. So, it was identified: hematite (α-Fe_2O_3), magnetite (Fe_3O_4), goethite (FeO.OH), chromite ($FeCr_2O_4$), roaldite (Fe_4N) and the iron nitride FeN. These results are consistent with the simulated corrosion products; where carburization did not occur, but nitridation does.

3.2.5 Kinetic study

The kinetic study observed in Figure 7, allowed to determinate the protective character of the oxide layer formed on P91 steel in the combustion environment. Thus, it was found that the kinetic behavior of the oxide layer was

not perfectly parabolic, but very close to it. Such behavior is typical of oxide layers where the diffusive processes slows down over time. When comparing the kinetic constants obtained in this work, with those reported by Alviz, et al. (2017) in their study of pure oxidation, a high similarity was found, which is related to similar experimental conditions and with the fact that only oxidation was obtained. These results are an indication that there was no catastrophic oxidation for the times evaluated, ruling out the formation of internal carbides. Finally, it was observed that kinetic constants varied in quadratic form with the increase in temperatures.

4. Conclusions

Starting from a representative mixture of refinery gases and a steel commonly used in equipment that works at high temperatures at the industry, a combustion environment was simulated to evaluate corrosive effects. Among the main results found, the carburization phenomenon was not identified, but instead it was possible to obtain a layer of duplex oxide, with surface nitrides. The oxide layer was mainly composed of Fe_2O_3, Fe_3O_4 and $FeCr_2O_4$; results that were consistent with the simulation performed. On the other hand, the formation kinetics of the oxide layers suggested the presence of semi-protective oxide layers, indicating that after 200 h in range of temperatures between 450 and 750ºC, the combustion environment in a refinery could not cause significant physical changes on P91 steel. Where, as the physical analysis showed in this work, it is possible to obtain the precipitation of carbides type $M_{23}C_6$ and M_7C_6 in the metallic matrix, with a ferritic microstructure rich in lamellar perlite, which slightly increases the microhardness of the alloy, but with a constant hardness.

Acknowledgments

The authors express their acknowledgments to the Administrative Department of Science, Technology and Innovation of Colombia (COLCIENCIAS) and Colombian Network of Knowledge in Energy Efficiency (RECIEE) for financial support of this work, that is part of the project “Consolidation of the knowledge network on energy efficiency and its impact on the productive sector under international standards - Design of a methodology for the eco-efficient management of combustion processes, case study: the oil refining industry” code of COLCIENCIAS: 110154332086.

References

Alviz, A., Kafarov, V., Meriño L., 2017a, Methodology for evaluation of corrosion damage during combustion process in refinery and petrochemical industry. case study: AISI 304 and astm A335 P5 steels, Chemical Engineering Transactions, 61, 1315-1320.

Alviz, A., Kafarov, V., Peña-Ballesteros, D., 2017b, Study of the continuous corrosion in an oxidation environment derived from the theoretical combustion products in a refinery. Case study: Ferritic steel ASTM A335 P91, IOP Conf. Series: Journal of Physics, 935, 1-7.

American Society for Testing and Materials, 2011, Standard Practice for Preparing, Cleaning, and Evaluating Corrosion Test Specimens (ASTM G1-03 ed.). United States: ASTM International.

Aspen HYSYS (version 8.6) [software], 2014, obtained from <www.aspentech.com/en/resources/press-releases/aspentech-introduces-aspenonert-version-8-6-software2147490592> accessed 28-05-18.

HSC Chemistry (version 5.1) [software], 2002, obtained from <hsc-chemistry.software.informer.com/5.1/.> accessed 28-05-18.

John, R., 2010, Sulfidation and mixed gas corrosion of alloys. Shreir’s Corrosion, 240–271.

Kafarov, V., Toledo, M., & Meriño, L., 2015, Numerical Simulation of Combustion Process of Fuel Gas Mixtures at Refining Industry, Chemical Engineering Transactions, 43, 1351–1356.

Martinelli, L., Desgranges, C., Rouillard, F., Ginestar, K., Tabarant, N., Rousseau, K., 2015, Comparative oxidation behaviour of Fe-9Cr steel in CO_2 and H_2O at 550ºC: Detailed analysis of the inner oxide layer, Corrosion Science, 100, 253-266.

Peña-Ballesteros, D., Vásquez-Quintero, C., Laverde-Cataño, D., Serna-Gil, A., 2012, High temperature corrosion of 9Cr-1Mo ferritic steel P91 modified, in oxidizing-carburizing atmospheres, Revista de Metalurgia, 48, 97–106.

Pérez, F., Castañeda, S., 2006, Study by Means of the Mass Spectrometry of Volatile Species in the Oxidation of Cr, Cr2O3, Al, Al2O3, Si, SiO2, Fe and Ferritic/Martensitic Steel Samples at 923 K in Ar+(10 to 80%)H2O Vapor Atmosphere for New-Materials Design, Oxidation of Metals, 66, 231–251.

Rouillard, F., Furukawa, T., 2016, Corrosión of 9-12Cr ferritic-martensitic steels in high temperature CO_2, Corrosion Science, 105, 120–132.

Saavedra, J., Merino, L., Kafarov, V., 2013, Computer aided evaluation of eco-efficiency of refinery combustion process. Chemical Engineering Transactions, 32, 217–222.